Mobility Reversal of Polyelectrolyte-Grafted Colloids in Monovalent Salt Solutions

Shervin Raafatnia,[†] Owen A. Hickey,[‡] and Christian Holm[*]
Institut für Computerphysik, Universität Stuttgart, Allmandring 3, D-70569 Stuttgart, Germany
(Received 29 April 2014; revised manuscript received 11 July 2014; published 2 December 2014)

We present molecular dynamics simulations on the electrophoresis of a negative colloid grafted with positive polyelectrolytes. Net-neutral colloids show a varying mobility in monovalent salt. For colloids with negative net charge the mobility is negative at low and positive at high salt concentrations. This mobility reversal is an electrokinetic effect, and thus different from that observed in multivalent salt. Our results agree with numerical calculations based on the Darcy-Brinkman formalism, with which we predict the mobility reversal to also occur for experimentally accessible colloids.

DOI: 10.1103/PhysRevLett.113.238301 PACS numbers: 82.70.Dd, 47.57.jd, 82.35.Rs, 87.15.Tt

Polymers and colloids typically become ionized in aqueous solutions. The charged nature of these objects has made electrophoresis, the movement of a charged particle in solution subject to an electric field, into one of the main tools for their characterization. The quantity measured experimentally is the electrophoretic mobility μ, the ratio of the drift speed v to the applied electric field strength E, and it is independent of the field strength at low fields.

The electrophoresis of bare particles of different shapes and surface charges, such as DNA, spherical colloids, and flat surfaces, has been extensively studied. Recently, specific attention was paid to the phenomenon of mobility reversal as a function of the ionic strength. This mobility reversal is limited to multivalent counterions and high surface charge densities and salt concentrations [1–11]. The necessary charge inversion is caused by the strong correlations of the multivalent counterions and does not occur with monovalent salt ions.

The electrokinetic properties of polyelectrolyte-coated spheres (here referred to as soft colloids) are significantly more complex due to the nonuniform surface charge distribution and the polymers' hydrodynamic drag [12–16]. These effects must be taken into account to model the electrophoresis of biological cells, which often have naturally occurring polymer coatings [17–22]. In addition, artificial polymer coatings are used to control the electrokinetic properties of surfaces [23–25], rheological properties of electrorheological fluids [26,27], and the stability of colloidal suspensions [28]. Soft colloids also show great promise as drug and gene delivery vehicles [29–31]. The broad range of applications has generated extensive theoretical, numerical, and experimental work on this topic [13,14,20,28,32–40].

We report on molecular dynamics (MD) simulations of the electrophoresis of negative colloids grafted with positive polymers in the presence of monovalent salt of varying concentration. We investigate the mobility for two distinct cases. The first case is a net-neutral soft colloid, i.e., the core's charge is exactly balanced by the charges on the polyelectrolytes. In the second case, the magnitude of the core's charge is larger than the charges on the brush and thus the soft colloid has a net negative charge. Interestingly, the neutral soft colloid has a positive mobility at moderate and high salt concentrations. When it has a negative net charge, there is a mobility reversal as a function of *monovalent* salt concentration. This supports the theoretical prediction that at high salt concentrations the mobility of a soft particle is governed by the properties of the grafted layer [32,41,42]. The physical origin of the mobility reversal reported here is different from that of the bare surfaces as it does not rely on the strong correlations of multivalent salt. We explain these results by examining the radial monomer and ion density profiles and comparing the two important length scales of the system, namely, the Debye length λ_D and the polymer layer's thickness H. We obtain good agreement between our simulations and numerical calculations using an extended version of the standard electrokinetic model [42], which takes into account both the fixed charges on the brush and its hydrodynamic drag. The numerical calculations show that the above-mentioned mobility reversal also occurs for experimentally relevant colloid sizes.

We use the Extensible Simulation Package for Research on Soft Matter (ESPResSo) [43,44] to simulate a soft colloid in the canonical (NVT) ensemble. The simulations are carried out in a cubic box of length $L = 48\sigma$ with periodic boundary conditions, σ being the MD length unit introduced below. Our model consists of spherical beads to represent all particles, as shown in the snapshots at the top of Fig. 1. Steric repulsion between the beads results from the Weeks-Chandler-Anderson (WCA) potential [45]:

$$V_{\mathrm{WCA}}(r) = \begin{cases} 4\varepsilon\left[\left(\frac{\sigma}{r-r_o}\right)^{12} - \left(\frac{\sigma}{r-r_o}\right)^{6} + \frac{1}{4}\right] & r_o < r < 2^{1/6}\sigma + r_o \\ 0 & \text{elsewhere,} \end{cases} \quad (1)$$

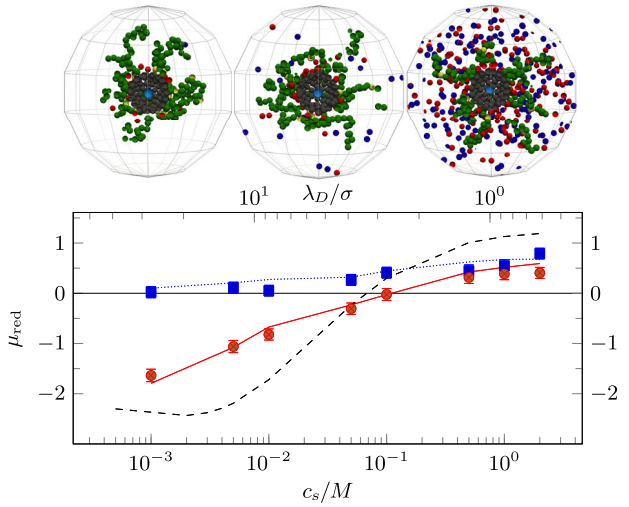

FIG. 1 (color online). Reduced mobility μ_{red} as a function of salt concentration c_s and the corresponding Debye length λ_D. Simulations for a neutral soft colloid (blue squared) and a charged soft colloid with $Q_{net} = -50e$ (red circles) are shown. Numerical results are depicted respectively by the dotted and solid lines of the same color. The dashed line shows the numerical result for a negatively charged soft colloid with the same core and net charge density as used for the red circles, but with $R_{col} = 1\mu m$. At the top three simulation snapshots are shown for the charged soft colloid at $c_s = \{0.001, 0.1, 1.0\}M$ respectively from left to right. These show only a radius of 14σ from the center of the colloid and are cut in half. The snapshots show the neutral monomers (green), charged monomers (yellow), positive salt ions (red), negative salt ions (dark blue), the surface raspberry beads (grey), and charged central colloid bead (light blue). The applied electric field is from left to right in these pictures.

where $\sigma \sim 3.5$ Å and $\varepsilon = k_BT$ (T is the temperature and $k_BT = 4.11$ pN nm $= 0.0256$ eV at room temperature) are the fundamental length and energy scales of the simulation, respectively. The offset is set to $r_o = 0$ except for interactions with the central bead of the colloid (introduced below), where it is $r_o = R_{col} = 3\sigma$. The colloid is based on the raspberry model [46–48], represented by one central bead surrounded by 113 surface beads a distance $R_{col} = 3\sigma$ from the center; see the snapshots at the top of Fig. 1. The raspberry is simulated as a rigid structure using the virtual sites feature of ESPResSo with mass $114m_0$, where $m_0 = 10^{-26}$ kg is the MD unit of mass, and the moment of inertia is $678m_0\sigma^2$, corresponding to a hollow spherical shell. $M = 20$ polyelectrolytes with $N = 20$ monomers are grafted to distinct surface beads. A minimum distance of 1.5σ between grafting beads creates a fairly uniform brush. The monomers are bonded together via the finitely extensible nonlinear elastic (FENE) potential

$$V_{FENE}(r) = -\frac{kR_0^2}{2}\ln\left[1 - \left(\frac{r}{R_0}\right)^2\right], \qquad (2)$$

where $R_0 = 1.5\sigma$ is the maximum bond distance and $k = 30\varepsilon/\sigma^2$ is the energy scale. The same potential is used to graft the polyelectrolytes to the colloid, except $R_0 = 2.0\sigma$.

A fraction $\lambda = 0.1$ of the 400 monomers are selected randomly and given a positive unit charge, the remainder are left uncharged. A negative charge Q_{col} is imparted on the central bead of the raspberry. We focus on two cases, $Q_{col} = -40e$ and $Q_{col} = -90e$, leading to net charges $Q_{net} = 0e$ and $Q_{net} = -50e$, respectively. Monovalent counterions are added, if necessary, to neutralize the system along with a concentration c_s of monovalent salt ions. Electrostatic interactions are calculated using P3M [49,50] with Bjerrum length $l_B = 2\sigma = 7$ Å. An electric field $\vec{E} = (0.1\varepsilon/(e\sigma), 0, 0)$ is added as a constant force $q_i\vec{E}$ acting on every charged bead i with charge q_i. This electric field strength has been shown to be low enough to avoid strong nonlinear effects in E [47,51]. In addition, it is sufficiently small to prevent a significant polarization of the brush; see Figs. 1 and 2 of the Supplemental Material [52]. We use a time step of $\Delta t = 0.01\tau$, where $\tau = \sigma(m_0/\varepsilon)^{1/2}$ is the MD unit of time. All beads are coupled to ESPResSo's D3Q19 lattice-Boltzmann fluid [53] with a kinematic viscosity $\nu = 3\sigma^2/\tau$, grid spacing of $a = 1\sigma$, and density $\rho = 0.85m_0/\sigma^3$ resulting in a dynamic viscosity of $\eta = 2.55m_0/(\sigma\tau)$ [54–56], via the scheme described in Refs. [54,55] using a coupling constant $\Gamma = 20\sigma m_0/\tau$. The temperature is controlled via the lattice-Boltzmann thermostat with $k_BT = \varepsilon$. To calculate μ, we apply an electric field and simulate for 30 000 000 MD steps, considering the system to be in its steady state after 5 000 000 MD steps. We measure the drift velocity of the center of mass of the colloid and divide by $E = 0.1\varepsilon/(e\sigma)$. Here we report the reduced mobility $\mu_{red} = 3\eta e/(2\epsilon k_BT)\mu$, where ϵ is the permittivity of the solution.

We compare our results to numerical calculations using the program "mobility and polarizability for soft particles using the electro-kinetic transport equations" (MPEK-0.02) provided by Hill and described in Ref. [42]. This program is based on the O'Brien and White approach [57], extended for polymer-coated spheres and solves a Poisson-Nernst-Planck equation with an additional advective term combined with the Darcy-Brinkman equation:

$$\eta\nabla^2\vec{u}(\vec{r}) = \vec{\nabla}P(\vec{r}) - \frac{\eta}{l^2(\vec{r})}[\vec{v} - \vec{u}(\vec{r})] + \sum_{j=1}^{N_s} n_j(\vec{r})z_j e\vec{\nabla}\psi(\vec{r}). \qquad (3)$$

Here $\vec{u}$ is the velocity of the solvent, P is the pressure, N_s is the number of ion species, n_j and z_j are the concentration and valency of species j, respectively, and ψ is the electrostatic potential. l^2 is the permeability of the polymer layer and decreases with increasing local monomer density.

This diffuse polymer layer shields the electro-osmotic flow (EOF) generated by the penetrated ions through an additional friction force. The ion penetration is energetically favorable; while electrostatically attracted to the core or the charged monomers, their entropy is not drastically reduced.

The mobility as a function of ionic strength for both a neutral soft colloid $Q_{\text{net}} = 0e$ ($Q_{\text{col}} = -40e$) and a negative soft colloid $Q_{\text{net}} = -50\text{e}$ ($Q_{\text{col}} = -90\text{e}$) is plotted in Fig. 1. In the low salt limit, the mobility is zero for the neutral soft colloid and negative for the negative one, as expected. This is compatible with theoretical findings of Hill *et al.* [42]. At low salt concentrations, there are hardly any ions in the system, making λ_D longer than the characteristic dimensions of the colloid. In the Hückel limit of no salt, the mobility of a spherical particle is given by $\mu = Q_{\text{net}}/(6\pi\eta R_H)$, where R_H is the hydrodynamic radius of the object. While this explains the results for the neutral case, using it for our net-charged soft colloid with $R_H = R_{\text{col}} + 2R_G^{\perp} \sim 7\sigma$ gives $\mu_{\text{red}} \approx -15$, which is much larger than the simulation mobility at $c_s = 0.001$ M. $R_G^{\perp}$ is the component of the radius of gyration of polymers perpendicular to the core's surface with a value of $R_G^{\perp} \sim 2\sigma$ and $2R_G^{\perp}$ is a measure for H (data not shown). The high density of counterions near the colloid's surface in Fig. 2(d) shows that we are far from the Hückel limit. Because of the finite colloidal concentration, there is a significant number of counterions adjacent to the colloid reducing the mobility [58].

The mobility of the negatively charged soft colloid changes sign around $c_s = 0.1$ M. This corresponds to $\lambda_D \sim 3\sigma$, which is comparable to H. In Fig. 2 we see that the accumulation of counterions within the brush is significantly greater at $c_s = 0.1M$ compared to $c_s = 0.001M$. The EOF of these ions is strongly screened by the brush and thus does not reach the bulk, leading to increased mobilities. The accumulation of counterions within the brush with increasing salt concentration is most pronounced when $\lambda_D \approx H$. This causes the large increase in the mobilities when λ_D goes from being longer to shorter than H. At the highest salt concentration, $c_s = 2.0M$, the mobilities in Fig. 1 saturate at a finite value, in contrast to bare colloids where the mobility is negligible at high ionic strengths [59,60]. The mobilities are roughly equal regardless of the core's charge. This agrees with theoretical predictions for the mobility of soft surfaces at hight salt concentrations [24,25,33,41,42]. According to Ohshima *et al.* [32], in the limit of $\kappa \to \infty$ the mobility scales with the charge density of the polyelectrolytes λ as $\mu = ze\lambda/(6\pi\eta a_s)$, where a_s is the monomer radius. Taking $a_s = 0.3\sigma$ [55] results in $\mu_{\text{red}} \sim 0.6$, which agrees with our results.

We compared our results in Fig. 1 to numerical results of the extended electrokinetic model of Hill *et al.* [42] and found good quantitative agreement. For both $Q_{\text{net}} = 0e$ and $Q_{\text{net}} = -50e$, the slight differences between the numerical and simulation results are mostly due to the fits to the simulation monomer densities shown in Figs. 2(a) and 2(b), which are an input into the numerical calculations. The good agreement between simulated and numerical results confirms the validity and applicability of the Darcy-Brinkman equation to describe the electrokinetics of soft particles. To show that the reversal also occurs for experimentally realizable colloids at experimentally

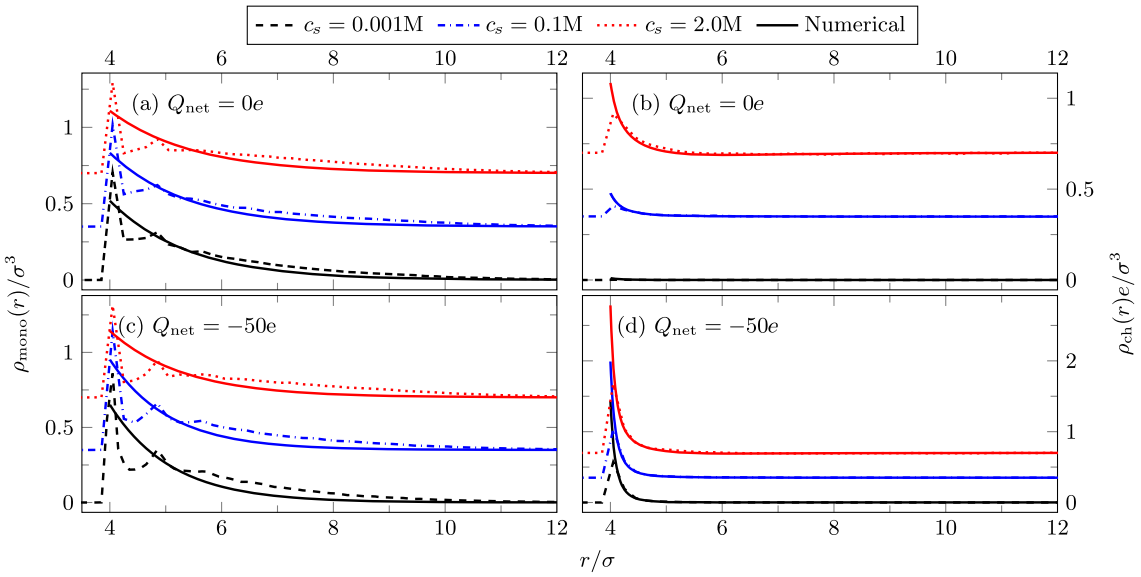

FIG. 2 (color online). Radial density profiles for $c_s = 0.001M$ (dashed black lines), $c_s = 0.1M$ (dash-dotted blue lines), and $c_s = 2M$ (dotted red lines) of the monomers $\rho_{\text{mono}}(r)$ and fluid charge, i.e., the sum of the ions' charges excluding the charges fixed on the polymers, $\rho_{\text{ch}}(r)$. Panels (a) and (b) show the data for the neutral soft colloid while panels (c) and (d) are for $Q_{\text{net}} = -50e$. All curves are shifted vertically by factors of 0.35. The solid lines represent the values produced by the program from Hill *et al.* [42].

accessible salt concentrations, we obtained numerical results for the same core and net surface charge densities as in the $Q_{\mathrm{net}} = -50e$ simulations, except with a much larger radius $R_{\mathrm{col}} \approx 1$ μm. This is done by using the brush parameters obtained by a fit to one of the simulation monomer density profiles ($c_s = 0.001M$) for many different salt concentrations. Small variations in these parameters do not change the result significantly. The results in Fig. 1 demonstrate that the phenomenon also occurs for colloids of typical experimental diameter, since the mechanism is independent of the colloid size and only depends on the ratio of λ_D to H.

It is known that the mobility of large bare colloids with high surface charge densities is nonmonotonic as a function of ζ potential or the ionic strength [57,61–63]. This is the cause of the maximum in absolute mobility value for the large colloid at low salt concentrations. The increased mobility in this regime is a result of larger colloid size, as shown by Vorwerg *et al.* [64]. The charge density of the polyelectrolytes is computed from the constraint $Q_{\mathrm{net}} = Q_{\mathrm{col}} + \lambda MN$. In the numerical approach, the total number of monomers MN is obtained by integrating the fit to the simulated monomer density mentioned in the previous paragraph. Because of the larger values of Q_{net} and Q_{col} (to keep the corresponding core and net charge densities the same), and the larger radius of the core, λ is larger than for the smaller colloid. This results in a higher mobility in the polyelectrolyte-dominated regime. The higher values of the mobility at the two extremities of the salt concentration range lead to an increased slope of the $\mu - c_s$ curve compared to the small soft colloid.

To conclude, we presented particle-based simulations on the electrophoresis of two soft colloids, one of which was overall charge neutral, whereas the other one had a net charge of $Q_{\mathrm{net}} = -50e$. We found that the neutral soft colloid displayed an increasing mobility, whereas the negative one experienced a mobility reversal with increasing monovalent salt concentration.

Previous theoretical works showed that in the thin Debye layer limit it is the polyelectrolytes' properties rather than the underlying surface that controls the electrophoretic behavior [13,14,32,41]. This is due to the aggregation of the core's counterions near the surface within the polymer brush, which screens their EOF and hence their contribution to the overall mobility. The mobility undergoes a transition from a net-charge-dominated regime at low ionic strengths to a brush-dominated regime at high ionic strengths. In fact, at the highest ionic strengths the mobility of the neutral soft colloid is almost equal to that of the highly negative one and its value agrees well with the analytical expression of Ohshima *et al.* [32]. This regime change causes the mobility reversal of the net-negative soft colloid with increasing monovalent salt concentration. While mobility reversal in multivalent salt is well known, we are unaware of any reports of mobility reversal in *monovalent* salt. These two types of mobility reversal are of completely different natures: the former is caused by charge inversion due to ion correlations [10,11,65], while such correlations are absent in monovalent salt solutions. In the latter case, the interplay between the EOF and the grafted brush causes the soft particle to electrophorese in opposite directions at low and high salt concentrations.

Moreover, numerical results obtained from Hill's solver [42] agreed well with our simulations. The work thus represents a confirmation of the applicability of the Darcy-Brinkman formalism [37] combined with a Poisson-Nernst-Planck equation including advection for modeling these systems. This is also relevant for other problems, such as Poiseuille flow in a polymer-coated channel, the electrically driven flow through a polymer-coated nanopore, or calculating the Stokes friction of a soft colloid.

While our simulations were done using a tiny colloid, numerical calculations demonstrate that the phenomenon also occurs at typical experimental colloid sizes. The reason is that the physical basis of the mobility reversal does not depend on the colloidal radius. In fact, we believe it should occur as long as the colloid and the grafted polyelectrolytes are oppositely charged and the brush height is of the same order of magnitude as the Debye length. This effect could potentially be used in applications such as a *local* salt concentration probe, determination of the brush height, or for microfluidic valves.

Financial support from the DFG through the collaborative center SFB 716, as well as under Grant No. Ho 1108/22-1, and the Volkswagen Foundation is gratefully acknowledged. The authors would like to thank Georg Rempfer, Dr. Joost de Graaf, and Professor Reghan J. Hill for many fruitful discussions. We are also grateful to Professor Hill for providing the program used in the numerical calculations.

*Corresponding author.
holm@icp.uni-stuttgart.de
†shervin@icp.uni-stuttgart.de
‡ohickey@icp.uni-stuttgart.de

[1] M. Elimelech and C. R. O'Melia, Colloids Surf. **44**, 165 (1990).
[2] M. Quesada-Perez, A. Martin-Molina, F. Galisteo-Gonzalez, and R. Hidalgo-Alvarez, Mol. Phys. **100**, 3029 (2002).
[3] C. Labbez, A. Nonat, I. Pochard, and B. Jonsson, J. Colloid Interface Sci. **309**, 303 (2007).
[4] A. Martin-Molina, J. A. Maroto-Centeno, R. Hidalgo-Alvarez, and M. Quesada-Perez, Colloids Surf. A **319**, 103 (2008).
[5] C. Schneider, M. Hanisch, B. Wedel, A. Jusufi, and M. Ballauff, J. Colloid Interface Sci. **358**, 62 (2011).
[6] M. Tanaka and A. Y. Grosberg, Eur. Phys. J. E **7**, 371 (2002).
[7] P.-Y. Hsiao and E. Luijten, Phys. Rev. Lett. **97**, 148301 (2006).

[8] A. Diehl and Y. Levin, J. Chem. Phys. **125**, 054902 (2006).
[9] A. Kubíčková, T. Křížek, P. Coufal, M. Vazdar, E. Wernersson, J. Heyda, and P. Jungwirth, Phys. Rev. Lett. **108**, 186101 (2012).
[10] I. Semenov, S. Raafatnia, M. Sega, V. Lobaskin, C. Holm, and F. Kremer, Phys. Rev. E **87**, 022302 (2013).
[11] S. Raafatnia, O. A. Hickey, M. Sega, and C. Holm, Langmuir **30**, 1758 (2014).
[12] H. Ohshima, J. Colloid Interface Sci. **233**, 142 (2001).
[13] R. J. Hill and D. A. Saville, Colloids Surf. A **267**, 31 (2005).
[14] H. Ohshima, Colloid Polym. Sci. **285**, 1411 (2007).
[15] N. Houbenov, S. Minko, and M. Stamm, Macromolecules **36**, 5897 (2003).
[16] L. Rosen and D. Saville, J. Colloid Interface Sci. **149**, 542 (1992).
[17] H. Hayashi, S. Tsuneda, A. Hirata, and H. Sasaki, Colloids Surf. B **22**, 149 (2001).
[18] A. J. de Kerchove and M. Elimelech, Langmuir **21**, 6462 (2005).
[19] K. Makino and H. Ohshima, Sci. Tech. Adv. Mater. **12**, 023001 (2011).
[20] J. F. Duval and F. Gaboriaud, Curr. Opin. Colloid Interface Sci. **15**, 184 (2010).
[21] S. Levine, M. Levine, K. Sharp, and D. Brooks, Biophys. J. **42**, 127 (1983).
[22] R. Bos, H. C. van der Mei, and H. J. Busscher, Biophys. Chem. **74**, 251 (1998).
[23] H. J. Kaper, H. J. Busscher, and W. Norde, J. Biomater. Sci., Polym. Ed. **14**, 313 (2003).
[24] G. Danger, M. Ramonda, and H. Cottet, Electrophoresis **28**, 925 (2007).
[25] O. A. Hickey, C. Holm, J. L. Harden, and G. W. Slater, Macromolecules **44**, 9455 (2011).
[26] I. S. Lee, M. S. Cho, and H. J. Choi, Polymer **46**, 1317 (2005).
[27] Y. D. Kim and D. H. Park, Synth. Met. **142**, 147 (2004).
[28] T. L. Doane, C.-H. Chuang, R. J. Hill, and C. Burda, Acc. Chem. Res. **45**, 317 (2012).
[29] V. P. Torchilin, AAPS J. **9**, E128 (2007).
[30] K. Y. Win and S.-S. Feng, Biomaterials **26**, 2713 (2005).
[31] V. Toncheva, M. A. Wolfert, P. R. Dash, D. Oupicky, K. Ulbrich, L. W. Seymour, and E. H. Schacht, Biochim. Biophys. Acta **1380**, 354 (1998).
[32] H. Ohshima, M. Nakamura, and T. Kondo, Colloid Polym. Sci. **270**, 873 (1992).
[33] H. Ohshima, Curr. Opin. Colloid Interface Sci. **18**, 73 (2013).
[34] R. J. Hill, D. Saville, and W. Russel, J. Colloid Interface Sci. **263**, 478 (2003).
[35] T. L. Doane, Y. Cheng, A. Babar, R. J. Hill, and C. Burda, J. Am. Chem. Soc. **132**, 15 624 (2010).
[36] J. López-García, C. Grosse, and J. Horno, J. Colloid Interface Sci. **265**, 327 (2003).
[37] S. S. Dukhin, R. Zimmermann, J. F. Duval, and C. Werner, J. Colloid Interface Sci. **350**, 1 (2010).
[38] A. C. Barbati and B. J. Kirby, Soft Matter **8**, 10598 (2012).
[39] J. F. L. Duval and H. Ohshima, Langmuir **22**, 3533 (2006).
[40] D. Saville, J. Colloid Interface Sci. **222**, 137 (2000).
[41] J. L. Harden, D. Long, and A. Ajdari, Langmuir **17**, 705 (2001).
[42] R. Hill, D. Saville, and W. Russel, J. Colloid Interface Sci. **258**, 56 (2003).
[43] H. J. Limbach, A. Arnold, B. A. Mann, and C. Holm, Comput. Phys. Commun. **174**, 704 (2006).
[44] A. Arnold, O. Lenz, S. Kesselheim, R. Weeber, F. Fahrenberger, D. Röhm, P. Košovan, and C. Holm, in *Meshfree Methods for Partial Differential Equations VI*, Lecture Notes in Computational Science and Engineering Vol. 89, edited by M. Griebel and M. A. Schweitzer (Springer, Heidelberg, 2013), pp. 1–23.
[45] J. D. Weeks, D. Chandler, and H. C. Andersen, J. Chem. Phys. **54**, 5237 (1971).
[46] V. Lobaskin and B. Dünweg, New J. Phys. **6**, 54 (2004).
[47] V. Lobaskin, B. Dünweg, and C. Holm, J. Phys. Condens. Matter **16**, S4063 (2004).
[48] B. Dünweg, V. Lobaskin, K. Seethalakshmy-Hariharan, and C. Holm, J. Phys. Condens. Matter **20**, 404214 (2008).
[49] R. W. Hockney and J. W. Eastwood, *Computer Simulations Using Particles* (McGraw-Hill, New York, 1981).
[50] M. Deserno and C. Holm, J. Chem. Phys. **109**, 7678 (1998).
[51] K. Grass and C. Holm, Soft Matter **5**, 2079 (2009).
[52] See Supplemental Material at http://link.aps.org/supplemental/10.1103/PhysRevLett.113.238301 for data showing that polarization of the soft colloid is negligible.
[53] D. Röhm and A. Arnold, Eur. Phys. J. Spec. Top. **210**, 89 (2012).
[54] P. Ahlrichs and B. Dünweg, Int. J. Mod. Phys. C **09**, 1429 (1998).
[55] P. Ahlrichs and B. Dünweg, J. Chem. Phys. **111**, 8225 (1999).
[56] K. Grass, U. Böhme, U. Scheler, H. Cottet, and C. Holm, Phys. Rev. Lett. **100**, 096104 (2008).
[57] R. W. O'Brien and L. R. White, J. Chem. Soc., Faraday Trans. 2 **74**, 1607 (1978).
[58] H. Ohshima, J. Colloid Interface Sci. **248**, 499 (2002).
[59] S. S. Dukhin, R. Zimmermann, and C. Werner, J. Colloid Interface Sci. **313**, 676 (2007).
[60] H. Ohshima, Colloids Surf. A **103**, 249 (1995).
[61] M. Antonietti and L. Vorwerg, Colloid Polym. Sci. **275**, 883 (1997).
[62] M. Borkovec, S. H. Behrens, and M. Semmler, Langmuir **16**, 5209 (2000).
[63] A. S. Khair and T. M. Squires, Phys. Fluids **21**, 042001 (2009).
[64] L. Vorwerg, M. Antonietti, and K. Tauer, Colloids Surf. A **150**, 129 (1999).
[65] A. G. Moreira and R. R. Netz, Europhys. Lett. **52**, 705 (2000).